ReneSANCe event generator status and plans

V. Yermolchyk
on befalf of SANC team

JINR; INP BSU

The 2023 International Workshop on the High Energy Circular
Electron Positron Collider

24 October 2023

SANC – Support of Analitic and Numeric Calculations for experiments at colliders

> SANC –
> CEPC, Belle2, LHC, FCC, ILC, CLIC, ...

⇑

> μela –
> analysis of μe scattering data from the beam
> polarimeter of the SMC experiment at CERN

⇑

> HECTOR and polHECTOR –
> theoretical support for HERA

⇑

> ZFITTER –
> theoretical support for LEP-I and LEP-II
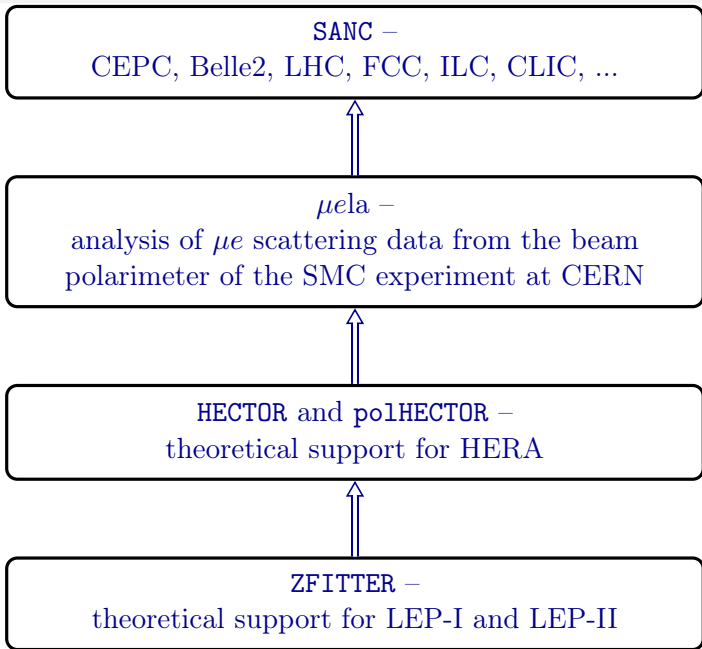
The SANC framework and products family

```
┌─────────────────┐      ┌─────────────────┐      ┌─────────────────┐
│   Analytical    │      │    FORTRAN      │      │     MCSANC      │
│     FORM        │ ═══▷ │    modules      │ ═══▷ │    MCSANCee     │
│  expressions    │      │  EW corrections │      │    SANCphot     │
│                 │      │                 │      │   integrators   │
└─────────────────┘      └─────────────────┘      └─────────────────┘
                                  ║
                                  ▽
                         ┌─────────────────┐
                         │    ReneSANCe    │
                         │    generator    │
                         └─────────────────┘
```
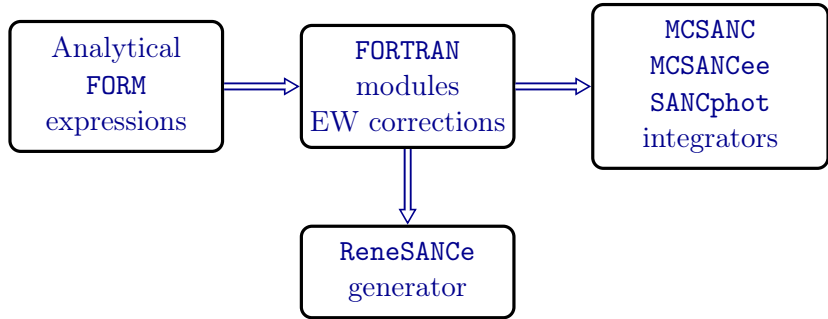
Publications:

SANC – CPC 174 481-517
MCSANC – CPC 184 2343-2350; JETP Letters 103, 131-136
SANCphot – arXiv:2201.04350
ReneSANCe – CPC 256 107445; CPC 285 108646

SANC products are available at http://sanc.jinr.ru/download.php
ReneSANCe is also available at http://renesance.hepforge.org

SANC advantages:

- full one-loop electroweak corrections
- higher order corrections
- massive case
- accounting for polarization effects
- full phase space operation
- results of ReneSANCe event generator and SANC integrators are thoroughly cross checked

Higher order improvements

Higher order corrections

QED corrections
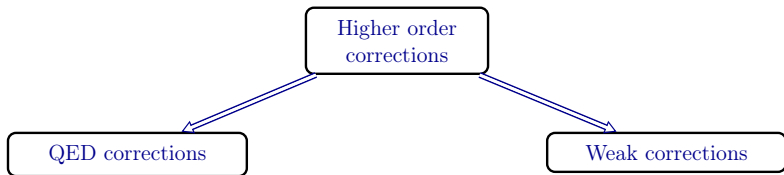
Weak corrections

- Leading logarithmic (LL) approximation.
- Corrections through $\Delta\alpha$.
- Shower with matching.

- Corrections through $\Delta\rho$.
- Leading Sudakov logarithms.

Higher order improvements, QED

Basic formula:

$$\sigma^{\text{LLA}} = \int\limits_0^1 dx_1 \int\limits_0^1 dx_2 \mathcal{D}_{ee}(x_1)\mathcal{D}_{ee}(x_2)\sigma_0(x_1, x_2, s)\Theta(\text{cuts}),$$

where $\sigma_0(x_1, x_2, s)$ – is the Born level cross section of the annihilation process with changed momenta of initial particles.

$\mathcal{D}_{ee}(x)$ describes the probability density of finding an electron with an energy fraction x in the initial electron beam.

[Kuraev, E.A.; Fadin, V.S. Sov. J. Nucl. Phys. 1985, 41, 466–472]

Higher order improvements, QED

The leading log is $L = \ln \frac{s}{m_l^2}$.

LO	1		
NLO	αL	α	
NNLO	$\frac{1}{2}\alpha^2 L^2$	$\frac{1}{2}\alpha^2 L$	$\frac{1}{2}\alpha^2$
N^3LO	$\frac{1}{6}\alpha^3 L^3$	$\frac{1}{6}\alpha^3 L^2$	...

In the LL approximation we can separate pure photonic (marked ``$\gamma$'') and the rest corrections which include pure pair and mixed photon-pair effects (marked as ``pair'').

$e^+e^- \to ZZ$, $\sqrt{s}$ =250, 500 and 1000 GeV

Multiple photon ISR relative corrections δ (%) in the LLA approximation.

$\sqrt{s}$, GeV	250	500	1000
$\mathcal{O}(\alpha L)$, γ	$-2.436(1)$	$+8.074(1)$	$+13.938(1)$
$\mathcal{O}(\alpha^2 L^2)$, γ	$-0.692(1)$	$-0.268(1)$	$+0.229(1)$
$\mathcal{O}(\alpha^2 L^2)$, e^+e^-	$-0.013(1)$	$+0.324(1)$	$+1.516(1)$
$\mathcal{O}(\alpha^2 L^2)$, $\mu^+\mu^-$	$-0.008(1)$	$+0.199(1)$	$+0.958(1)$
$\mathcal{O}(\alpha^3 L^3)$, γ	$+0.034(1)$	$-0.014(1)$	$-0.016(1)$
$\mathcal{O}(\alpha^3 L^3)$, e^+e^-	$-0.017(1)$	$-0.022(1)$	$-0.051(1)$
$\mathcal{O}(\alpha^3 L^3)$, $\mu^+\mu^-$	$-0.010(1)$	$-0.013(1)$	$-0.033(1)$
$\mathcal{O}(\alpha^4 L^4)$, γ	< 0.001	< 0.001	< 0.001

$e^+e^- \rightarrow t\bar{t}$, $\sqrt{s} =$ 350 and 500 GeV

Multiple photon ISR relative corrections δ (%) in the LLA approximation.

$\sqrt{s}$, GeV	350	500
$\mathcal{O}(\alpha L)$, γ	$-42.546(1)$	$-3.927(1)$
$\mathcal{O}(\alpha^2 L^2)$, γ	$+8.397(1)$	$-0.429(1)$
$\mathcal{O}(\alpha^2 L^2)$, e^+e^-	$-0.460(1)$	$-0.030(1)$
$\mathcal{O}(\alpha^2 L^2)$, $\mu^+\mu^-$	$-0.277(1)$	$-0.018(1)$
$\mathcal{O}(\alpha^3 L^3)$, γ	$-0.984(1)$	$+0.021(1)$
$\mathcal{O}(\alpha^3 L^3)$, e^+e^-	$+0.182(1)$	$-0.012(1)$
$\mathcal{O}(\alpha^3 L^3)$, $\mu^+\mu^-$	$+0.110(1)$	$-0.008(1)$
$\mathcal{O}(\alpha^4 L^4)$, γ	$+0.070(1)$	$+0.002(1)$

DGLAP

Dokshitzer–Gribov–Lipatov–Altarelli–Parisi (DGLAP) evolution
equation:

$$Q^2 \frac{\partial}{\partial Q^2} D(x, Q^2) = \frac{\alpha}{2\pi} \int_x^1 \frac{dy}{y} P_+(y) D(\frac{x}{y}, Q^2)$$

Sudakov form factor:

$$\Delta(s_1, s_2) = \exp[-\frac{\alpha}{2\pi} \int_{s_2}^{s_1} \frac{dQ^2}{Q^2} \int_0^{1-\epsilon} dy P(y)]$$

Energy distribution of electrons according shower algorithm
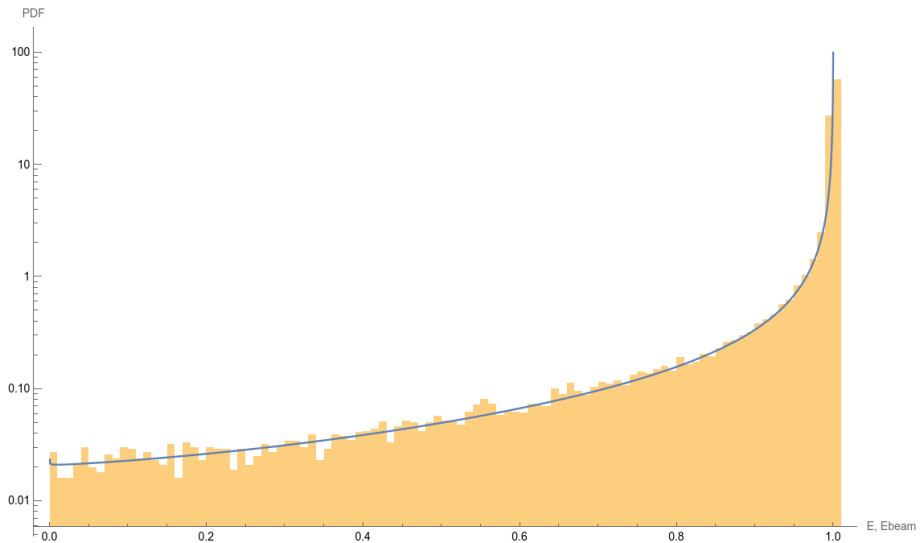
Higher order improvements, weak

Higher order improvements added to NLO cross section through $\Delta\rho$ parameter: $s_W^2 \to \bar{s}_W^2 \equiv s_W^2 + \Delta\rho\, c_W^2$.

$\mathcal{O}(\alpha)$ A. Sirlin, PRD22, (1980) 971, W.J. Marciano, A. Sirlin, PRD22 (1980) 2695; G. Degrassi, A. Sirlin, NPB352 (1991) 352, P. Gambino and A. Sirlin, PRD49 (1994) 1160

$\mathcal{O}(\alpha\alpha_s)$ A. Djouadi, C. Verzegnassi, PLB195 (1987) 265; B. Kiehl, NPB353 (1991) 567; B. Kniehl, A. Sirlin, NPB371 (1992) 141, PRD47 (1993) 883; A. Djouadi, P. Gambino, PRD49 (1994) 3499

$\mathcal{O}(\alpha\alpha_s^2)$ L. Avdeev et al., PLB336 (1994) 560;K.G. Chetyrkin, J.H. Kuhn, M. Steinhauser, PLB351 (1995) 331; PRL75 (1995) 3394; NPB482 (1996)

$\mathcal{O}(\alpha\alpha_s^3)$ Y. Schroder, M. Steinhauser, PLB622 (2005) 124; K.G. Chetyrkin et al., hep-ph/0605201; R. Boughezal, M. Czakon, hep-ph/0606232

$\mathcal{O}(\alpha^2)$ G. Degrassi, P. Gambino, A. Sirlin, PLB394 (1997) 188; M. Awramik, M. Czakon, A. Freitas, JHEP0611 (2006) 048

$e^+e^- \to t\bar{t}$, $\sqrt{s} =$ 350 and 500 GeV

Integrated Born and weak contributions to the cross section and higher-order leading corrections in two EW schemes: $\alpha(0)$ and G_μ.

$\sqrt{s}$, GeV	350	500
$\sigma_{\alpha(0)}^{\mathrm{Born}}$, pb	0.22431(1)	0.45030(1)
$\sigma_{G_\mu}^{\mathrm{Born}}$, pb	0.24108(1)	0.48398(1)
$\delta_{G_\mu/\alpha(0)}^{\mathrm{Born}}$, %	7.48(1)	7.48(1)
$\sigma_{\alpha(0)}^{\mathrm{weak}}$, pb	0.25564(1)	0.47705(1)
$\sigma_{G_\mu}^{\mathrm{weak}}$, pb	0.26055(1)	0.48420(1)
$\delta_{G_\mu/\alpha(0)}^{\mathrm{weak}}$, %	1.92(1)	1.50(1)
$\sigma_{\alpha(0)}^{\mathrm{weak+ho}}$, pb	0.25900(1)	0.48483(1)
$\sigma_{G_\mu}^{\mathrm{weak+ho}}$, pb	0.25986(1)	0.48289(1)
$\delta_{G_\mu/\alpha(0)}^{\mathrm{weak+ho}}$, %	0.33(1)	$-0.40(1)$

Processes of interest

- Bhabha ($e^+e^- \to e^-e^+$), Phys. Rev. D 98, 013001.
- ZH ($e^+e^- \to ZH$), Phys. Rev. D 100, 073002.
- s-channel ($e^+e^- \to \mu^-\mu^+$, $e^+e^- \to \tau^-\tau^+$), Phys. Rev. D 102, 033004.
- Photon-pair ($e^+e^- \to \gamma\gamma$), Phys. Rev. D 107, 073003.
- s-channel ($e^+e^- \to t\bar{t}$), Phys. Rev. D 107, 113006.
- Muon-electron scattering ($\mu^+e^- \to \mu^+e^-$), Phys. Rev. D 105, 033009.
- Møller ($e^-e^- \to e^-e^-$, $\mu^+\mu^+ \to \mu^+\mu^+$), JETP Lett. 115, 9.
- Zγ ($e^+e^- \to Z\gamma$).
- ZZ ($e^+e^- \to ZZ$).
- WW ($e^+e^- \to W^+W^-$).
- publication, available in release of the generator
- publication, in preparation for next release of the generator
- in preparation

Basic processes of SM for e^+e^- annihilation
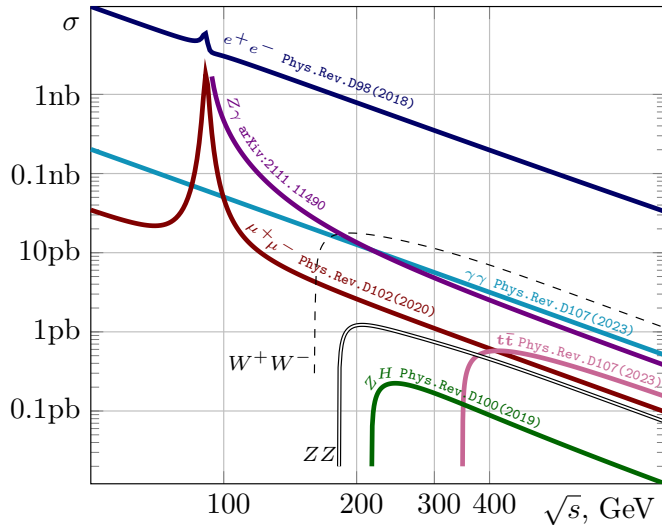
The cross sections are given for polar angles between $10^o < \theta < 170^o$ in the final state.

Distributions

For each process we provide all important distributions:

- Cross section over energy and angle distribution
- Asymmetries: Forward-Backward, Left-Right, ...
- Final-State Fermion Polarization

$e^+e^- \to ZH$, energy dependence

Pure weak (PW) and QED relative corrections in α_0 and G_μ EW-schemes.
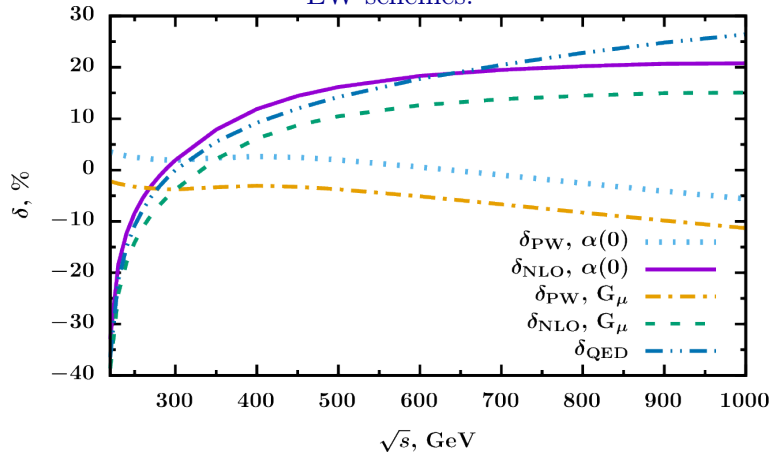
$e^+e^- \to t\bar{t}$, **energy dependence**

The LO and NLO EW corrected unpolarized cross sections and the relative corrections in parts as a function of the c.m.s. energy.
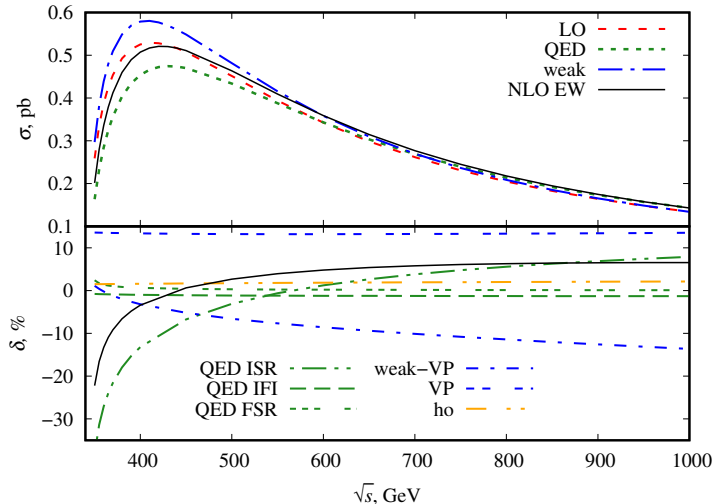
$e^+e^- \to t\bar{t}$, angle dependence

The left part corresponds to the unpolarized (black), and fully polarized, with $(P_{e^+}, P_{e^-} = +1, -1)$ (red) and $(-1, +1)$ (blue), initial beams, while the right one shows the partially polarized initial beams with $(P_{e^+}, P_{e^-} = (+0.3, -0.8)$ (red) and $(-0.3, +0.8)$ (blue) for the energy $\sqrt{s} = 350$ GeV.
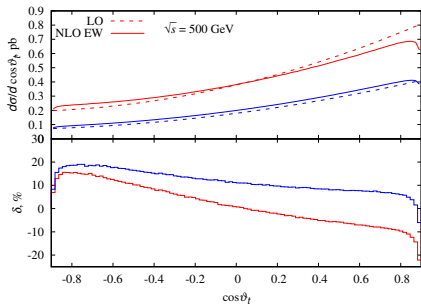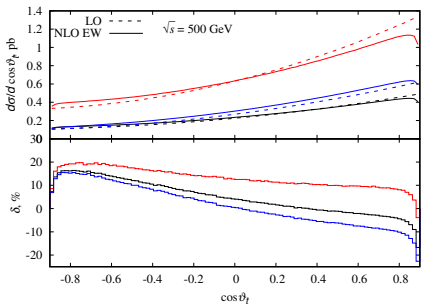
$e^+e^- \to \gamma\gamma$, Left–Right Asymmetry

Angular distributions for A_{LR} asymmetry over the highest energy photon angle $(\vartheta_{\gamma_{\mathrm{m}}})$ at several c.m. energies.
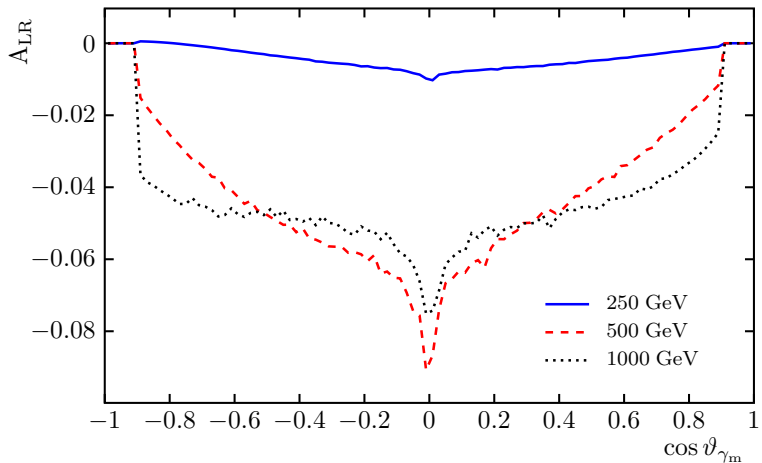
$e^+e^- \to \mu^+\mu^-$, **Left–Right Forward–Backward Asymmetry**
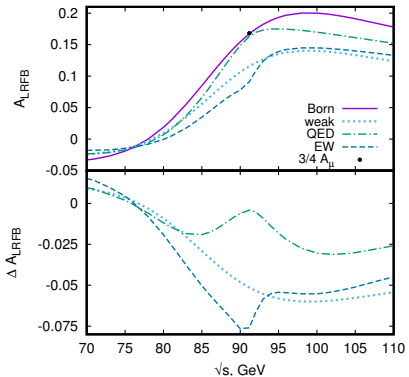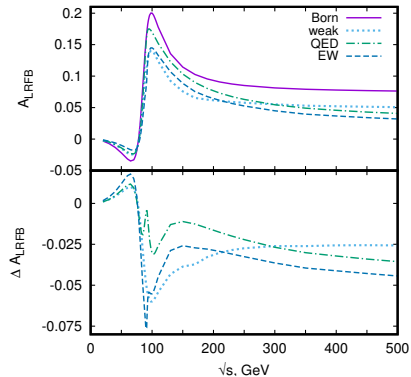
$e^+e^- \to \tau^+\tau^-$, **Final-State Fermion Polarization**
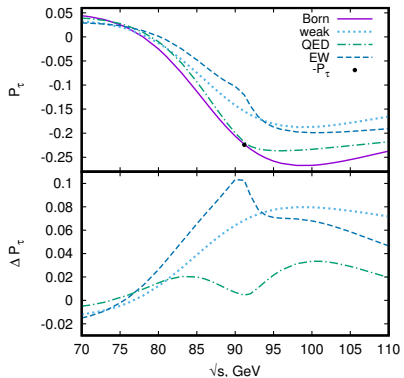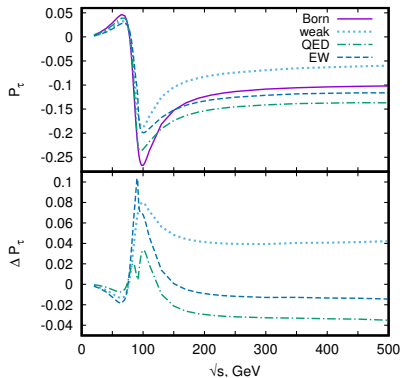
(**Left**) The P_τ polarization in the Born and 1-loop (weak, pure QED, and EW) approximations and ΔP_τ vs. c.m.s. energy in a wide range; (**Right**) the same for the Z peak region. The black dot indicates the value P_τ at the Z resonance.

Processes of interest

- $\gamma\gamma \to \gamma\gamma$
- $\gamma\gamma \to Z\gamma$
- $\gamma\gamma \to ZZ$
- $\gamma\gamma \to ZH$
- $\gamma\gamma \to \nu\bar{\nu}$
- $\gamma\gamma \to l^-l^+$
- $\gamma\gamma \to W^-W^+$

First step to transversal polarization.

Photon collider based on linear *ee* collider

$e \rightarrow \gamma$ conversion through the Compton scattering of laser light on high-energy electrons (I. Ginzburg, G. Kotkin, Phys.Part.Nucl. 52 (2021) 5, 899-912):
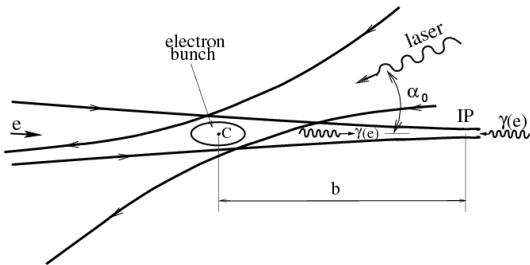
Basic parameters:

- $x_0 = \frac{4E\omega_0}{m_e^2}$, where E - electron energy, ω_0 - the laser photon energy

- P_e - electron beam long. polarization, P_γ - laser beam circular polarization, P_t - laser beam linear polarization, Φ - azimuthal angle of lazer photon linear polarization

- $y = \frac{\omega}{E}$, where ω - energy of the back-scattered photon

Density matrices for backscattered photons

$$\rho \quad = 1/2 \begin{pmatrix} 1 + \xi_2(y) & -\xi_{13}(y)e^{-2i(\Phi-\phi)} \\ -\xi_{13}(y)e^{2i(\Phi-\phi)} & 1 - \xi_2(y) \end{pmatrix},$$

$$\rho^{'} \quad = 1/2 \begin{pmatrix} 1 + \xi_2^{'}(y) & -\xi_{13}^{'}(y)e^{2i(\Phi^{'}-\phi)} \\ -\xi_{13}^{'}(y)e^{-2i(\Phi^{'}-\phi)} & 1 - \xi_2^{'}(y) \end{pmatrix}$$

$$\xi_2(y) = \frac{P_e f_2(y) + P_\gamma f_3(y)}{C(y)}, \quad \xi_{13}(y) = \frac{2r^2(y)P_t}{C(y)}, \quad C(y) = f_0(y) + P_e P_\gamma f_1(y)$$

$$f_0(y) = \frac{1}{1+y} + 1 - y - 4r(1-r),$$

$$f_1(y) = \frac{y}{1-y}(1-2r)(2-y),$$

$$f_2(y) = x_0 r[1 + (1-y)(1-2r)^2],$$

$$f_3(y) = (1-2r)(\frac{1}{1-y} + 1 - y),$$

$$r(y) = \frac{y}{x_0(1-y)}$$

Distributions for $\gamma\gamma \to ZZ$ ($\rho = 1$)
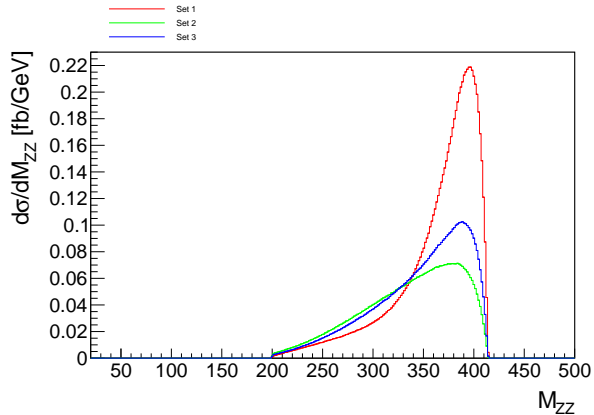
where ρ is the reduced distance between conversion and collision points (Ginzburg I. F., Kotkin G. L. Phys. J. C. 2000. V. 13. P. 295):

$$\rho^2 = \left(\frac{b}{\gamma\sigma_{xe}}\right)^2 + \left(\frac{b}{\gamma\sigma_{ye}}\right)^2$$

Polarization configurations:

- Set 1: $P_e = P_r^{'} = 0.8, P_\gamma = P_\gamma^{'} = -1, P_t = P_t^{'} = 0$
- Set 2: $P_e = P_r^{'} = 0, P_\gamma = P_\gamma^{'} = 0, P_t = P_t^{'} = 1, \Phi = \Phi^{'} = \pi/2$
- Set 3: $P_e = 0.8, P_e^{'} = 0, P_\gamma - 1, P_\gamma^{'} = 0, P_t = 0, P_t^{'} = 1, \Phi = \pi/2$

RESUME: SANC

- **Monte Carlo tools of SANC provide:**
  - **Complete one-loop EW corrections**
  - **Initial & final state polarization support**
  - **Easy to investigate various asymmetries**
  - **LL-accuracy improvements to cross section**
  - **Higher order improvements throw $\Delta\rho$**
- **ReneSANCe provide:**
  - **Events with unit weights**
  - **Output in Standard Les Houches Format**
  - **Simple installation & usage**
- **The research is supported by grant of the Russian Science Foundation (project No. 22-12-00021)**